

Criticality of Vacancy-Induced Metal-Insulator Transition in Graphene

Shangduan Wu¹ and Feng Liu^{2,*}

¹*Department of Physics and Astronomy, University of Utah, Salt Lake City, Utah 84112, USA*

²*Department of Materials Science and Engineering,
University of Utah, Salt Lake City, Utah 84112, USA*

(Dated: November 9, 2018)

The criticality of vacancy-induced metal-insulator transition (MIT) in graphene is investigated by Kubo-Greenwood formula with tight-binding recursion method. The critical vacancy concentration for the MIT is determined to be $x_c \approx 0.053\%$. The scaling laws for transport properties near the critical point are examined showing several unconventional 2D localization behaviors. Our theoretical results have shed some new lights to the understanding of recent experiments in H-dosed graphene [Phys. Rev. Lett. **103**, 056404 (2009)] and of 2D disordered systems in general.

PACS numbers: 73.63.-b, 72.15.Rn, 71.55.-i, 81.05.ue

Graphene, a single atomic layer of graphite, has drawn much interest in the last few years [1]. Because of the linear dispersion relation near the Dirac point, many unconventional transport behaviors have been shown in the pristine 2D graphene [2–4]. On the other hand, defects and impurities are often present in graphene, so their effects on graphene transport properties are of significant scientific interests and practical implications. Vacancy, one of the natural defects present in graphene, as observed in experiment [5], has been a subject of intense theoretical study [6–12]. Vacancy is predicted to induce *quasi*-localized states in the vicinity of Fermi energy [6, 8, 10], leading to a metal-insulator transition (MIT). However, some fundamental properties, especially the criticality of the vacancy-induced MIT in graphene remains unclear. One important question is what is the critical vacancy concentration for MIT. Furthermore, what are the scaling laws characterizing the transport properties close to the critical point? The answers to these questions will help us not only to explain recent experiment results in graphene [13] but also to better understand, in general, localization and transport behaviors in 2D disordered systems.

In this Letter, we report a theoretical study of criticality of the vacancy-induced MIT in graphene. Most importantly, we determine the critical vacancy concentration for MIT to be $x_c \sim 0.053\%$, which may be compared to the experimentally observed critical H coverage of $\sim 0.08\%$ for the H-dosing-induced MIT in graphene [13]. We found that electrical conductivity σ_{xx} scales with the diffusion length L in a power-law, in contrast to the logarithmic scaling predicted for a conventional 2D localization behavior [14, 15]. Above x_c , there exists a mobility edge E_c defining a transition point of energy from the localized states to the extended states, and the transition is discontinuous as characterized by a *non-zero* minimum conductivity σ_{min} at E_c . σ_{min} is found to vary from 1 to $1.3e^2/h$, different from the universal value of $0.628e^2/h$ expected in a conventional 2D localization system [14]. Our results are consistent with the most salient

features of the H-dosing-induced MIT in graphene observed recently [13], suggesting that both vacancy and H belong to short-range disorder in graphene.

The graphene is described by the π -band, nearest-neighbor tight-binding Hamiltonian as

$$\hat{H} = \sum_{i,\alpha} \varepsilon_i |i\alpha\rangle \langle i\alpha| - \sum_{\langle i,j \rangle, \alpha} \gamma_{ij} |i\alpha\rangle \langle j\alpha|, \quad (1)$$

where i and j are the neighboring sites on the lattice, $\alpha = (\uparrow, \downarrow)$ is spin index. ε_i is the on-site energy set to zero, and $\gamma_{ij} = \gamma = 2.7$ eV is the hopping energy. To calculate the conductivity, the real-space recursion method [16] in Kubo-Greenwood formula is adopted, which has been proved to be a powerful tool in treating various disordered graphene systems [17, 18]. The DC conductivity σ_{xx} at zero temperature can be calculated as $\sigma_{xx}(E) = (e^2/S)\rho(E) \lim_{t \rightarrow +\infty} \mathcal{D}(E, t)$. Here S is area per atom. $\rho(E) = \text{Tr}[\delta(E - \hat{H})]$ is average density of states (ADOS). $\mathcal{D}(E, t)$ is diffusion coefficient, which is defined as $\mathcal{D}(E, t) = \frac{1}{t} \frac{\text{Tr}\{\hat{x} \cdot \hat{U}(t)^\dagger \delta(E - \hat{H}) \hat{x} \cdot \hat{U}(t)\}}{\text{Tr}[\delta(E - \hat{H})]}$, where \hat{x} is the x -component of the position operator, $\hat{U}(t) = \exp(-i\frac{\hat{H}t}{\hbar})$ is time evolution operator, and t is diffusion time. Periodic boundary conditions are used with a supercell sizes $L_x \approx 738$ nm and $L_y \approx 213$ nm. Vacancies are introduced simply by removing the atoms from the lattice [6, 8].

Figure 1 shows the time dependence of diffusion coefficient \mathcal{D} at Fermi energy ($E_F = 0.0$ eV) for different vacancy concentration (x) in the range of $x \geq 0.1\%$. The inset shows the behavior of \mathcal{D} at large time scale. Three main features are observed: (1) \mathcal{D} first increases linearly with time and reaches its maximum \mathcal{D}_{max} at a very short time, less than 5 fs. \mathcal{D}_{max} is much smaller than $\mathcal{D} = v_F^2 t$ for perfect graphene, where Fermi velocity $v_F = 3ta/2\hbar \approx c/300$. This means that the transport leaves the ballistic regime ($d\mathcal{D}/dt > 0$) quickly and enters the diffusive regime ($d\mathcal{D}/dt = 0$) due to vacancies. However, the diffusive regime is very short, without a

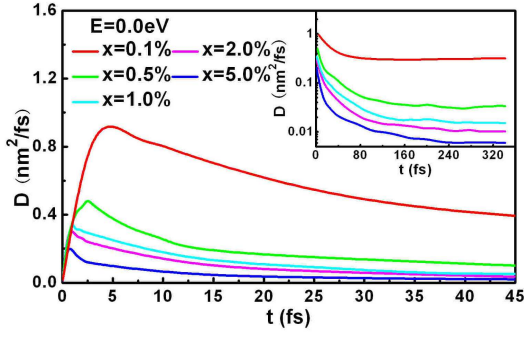


Figure 1: (Color online) Diffusion coefficient (\mathcal{D}) as a function of time (t) for different vacancy concentration (x) at E_F .

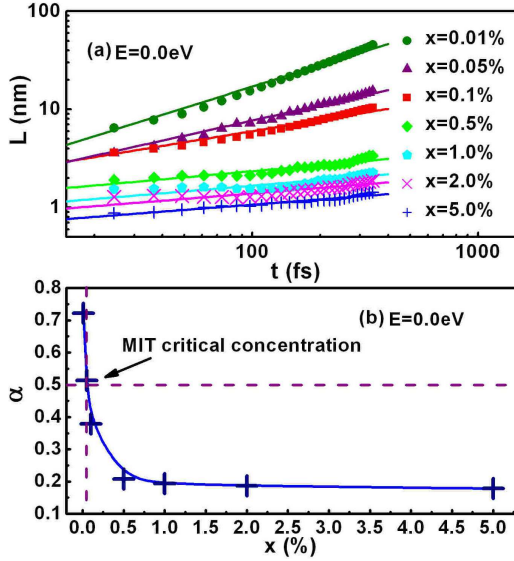


Figure 2: (Color online) (a) Diffusion length (L) as a function of time (t) for different vacancy concentration (x) at E_F . (b) Scaling exponent α as a function of vacancy concentration (x) at E_F .

plateau often seen in other systems. (2) Beyond \mathcal{D}_{max} , the system enters the localization regime, where \mathcal{D} decays in a power law $\mathcal{D} \propto t^{-\lambda}$, similar to the behavior of disordered carbon nanotube [19]. This indicates that the system stays in the localization regime ($d\mathcal{D}/dt < 0$) when $x \geq 0.1\%$ at large time scale, in agreement with the previous analytical results [6, 8, 10]. (3) \mathcal{D} decreases with the increasing x (inset of Fig. 1). This is because higher vacancy concentration leads to stronger scattering, reducing the diffusion coefficient. We note that at a given vacancy concentration, ρ is a constant independent of time. Therefore, the conductivity $\sigma_{xx} \sim \mathcal{D}\rho$ will have the same power-law scaling with time, $\sigma_{xx} \propto t^{-\lambda}$, as \mathcal{D} . Moreover, higher concentration will cause faster decay (larger λ) in both diffusion coefficient and conductivity.

The relationship between conductivity and diffusion length is very useful to better understand the transport behavior. By definition, $L(E, t) = \sqrt{\mathcal{D}(E, t)t}$, then we can easily find that $L \propto t^{\frac{1-\lambda}{2}} = t^\alpha$, which is verified for all the concentrations simulated, as shown in Fig. 2(a) with a Log-Log plot of diffusion length (L) versus time (t). Substituting t with L , σ_{xx} scales with L as $\sigma_{xx} \propto L^{\frac{2\alpha-1}{\alpha}}$. By dimensional analysis, σ_{xx} can be expressed as

$$\sigma_{xx}(L) = \sigma_0(e^2/h)(L/l)^{\frac{2\alpha-1}{\alpha}}, \quad (2)$$

where σ_0 is the conductivity in the diffusive regime in unit of e^2/h and l is the electron mean free path. It is important to note that such power-law dependence of conductivity on diffusion length is different from the usual logarithmic dependence, $\sigma(L) = \sigma_0 - (e^2/h\pi^2)\ln(L/l)$, as predicted by 2D scaling theory of localization [14]. We attribute this difference to the distinct nature of the *quasi*-localization induced by vacancies. The wave-function amplitude of the localized state induced by vacancies decays with the distance as $1/r$ [6, 8], which is not normalizable in 2D. Therefore, such *quasi*-localized state [6, 8] is different from the usual localized state, whose wave function decays exponentially with the distance [14].

It has been predicted that the vacancy-induced *quasi*-localization will lead to MIT in graphene [6, 8]. However, the critical vacancy concentration where the MIT occurs remains unknown. Here, we will determine the critical vacancy concentration for the MIT. From Fig. 2(a), we derive the scaling exponent, α , from the linear fitting of L versus t , and the resulting α are plotted as a function of x in Fig. 2(b). The curve of $\alpha(x)$ can be fit nicely by $L \propto t^{\frac{1-\lambda}{2}} = t^\alpha$, in the whole range of concentration. Notice that when $\alpha = 0.5$, $\lambda = 0$, then $d\mathcal{D}/dt = 0$ because $\mathcal{D} \propto t^{-\lambda}$, which means $\alpha = 0.5$ defines the position of diffusive regime. $\alpha > 0.5$ ($\lambda < 0$) means the ballistic regime and $\alpha < 0.5$ ($\lambda > 0$) means the localization regime. Thus, the power-law scaling holds true for all three transport regimes. α initially decreases rapidly with the increasing x , indicating the system quickly leaves the ballistic regime entering the localization regime. The transition point at $\alpha = 0.5$ defines the critical vacancy concentration for MIT, which is found to be $x_c \approx 0.053\%$ in Fig. 2(b). This value seems to agree quite well with the recent experimental result of critical concentration of MIT (0.08%) in H-dosed graphene [13]. It implies that similar transport behavior exists in these two disordered systems that both vacancy defect and H impurity create similar localization phenomena in graphene. In addition, the experiment suggested other unknown defects rather than H may induce MIT at even lower defect concentrations [13], which might be attributed, at least partly, to vacancies according to our calculation.

Next, we examine another criticality of the vacancy-induced MIT in graphene, the mobility edge (E_c), which

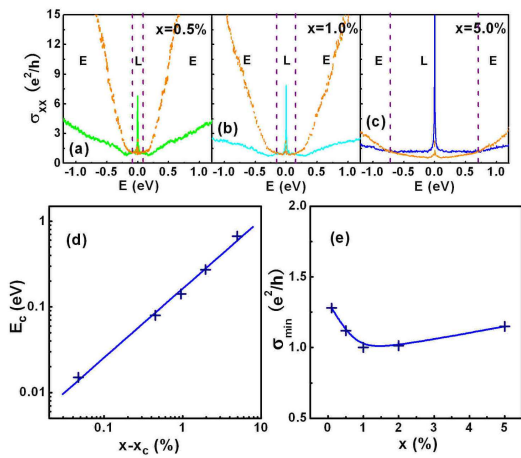


Figure 3: (Color online) (a), (b) and (c) Conductivity (σ_{xx}) as a function of energy (E) for vacancy concentration $x = 0.5\%$, $x = 1.0\%$ and $x = 5.0\%$ at the time t_1 when \mathcal{D} reaches its maximum (blue solid line) and $t_2 \approx 36.7$ fs (orange dash line). “E” indicates the extended state and “L” indicates the localized state. (d) The mobility edge (E_c) as a function of $x - x_c$. (e) The minimal conductivity (σ_{min}) at E_c as a function of x .

defines the critical energy where the system changes from the localized state to the extended state above the critical vacancy concentration x_c . We only need to consider $x > x_c$, because when $x < x_c$ the electronic states become extended over the whole energy range. Figures 3(a), (b) and (c) show the energy dependence of conductivity at two different times for three vacancy concentrations of 0.5%, 1.0%, and 5.0%, respectively. One time is chosen at where \mathcal{D} reaches its maximum, t_1 ($\mathcal{D} = \mathcal{D}_{max}$), and the other is chosen at a much later time ($t_2 \approx 36.7$ fs $\gg t_1$). At the low energies closed to E_F , $\sigma_{xx}(t_1) > \sigma_{xx}(t_2)$, but at the high energies away from E_F , $\sigma_{xx}(t_1) < \sigma_{xx}(t_2)$. This is because the low-energy electronic states are localized whose conductivity decreases with time; while the high-energy electronic states are extended whose conductivity increases with time. This is in qualitative agreement with the previous analysis of the inverse participation ratio (IPR) of electron wavefunction [6, 8]. Then, the mobility edge E_c can be obtained as the energy for $\sigma_{xx}(t_1) = \sigma_{xx}(t_2)$. In Figs. 3(a), (b) and (c), we see that the mobility edge E_c increases with the increasing vacancy concentration, as the increasing vacancy concentration expands the energy range of localization when $x > x_c$.

In Fig. 3(d), we plot E_c as a function of x , in a Log-Log scale, which clearly shows a power-law dependence of E_c on x . Fitting the simulation data, we obtain the scaling relation of $E_c \propto (x - x_c)^\beta$, with the scaling exponent $\beta \approx 0.81$. Importantly, a *non-zero* minimum conductivity σ_{min} appears at the mobility edge. Figure 3(e) shows that σ_{min} first decreases and then increases with

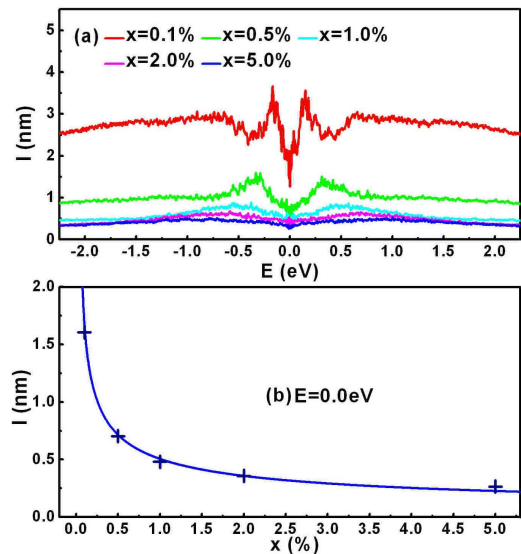


Figure 4: (Color online) (a) Mean free path (l) as a function of energy (E) for different vacancy concentration (x). (b) Mean free path (l) as a function of vacancy concentration (x) at E_F . The blue solid line is a fit to the data by $l \propto x^{-1/2}$.

x , but the reason for such trend is unclear. The existence of σ_{min} is possibly due to the *quasi*-localized nature of electronic states induced by vacancy in graphene. It indicates that the transition from the localized states to the extended states at the mobility edge is discontinuous as Mott argued [14], suggesting the break-down of one-parameter scaling theory. Also, our simulated σ_{min} varies from 1 to $1.3e^2/h$, different from the universal value of $0.628e^2/h$ as expected in conventional 2D localization system [14].

Last, we examine the electron mean free path l , an important length scale characterizing the degree of electron scattering by disorder. In Fig. 4(a), the energy dependence of l is shown, which is obtained by $l(E) = \mathcal{D}_{max}(E)/v(E)$ [19, 20]. $v(E)$ is the average wave-packet velocity at energy E , extracted from the diffusion coefficient in the ballistic regime at short times as $\mathcal{D}(E, t) \approx v(E)^2 t$. It is interesting to observe a minimal mean free path at E_F . This distinguishes vacancies from other disorders in graphene that give rise to a maximal mean free path at E_F [17, 18]. The minimal mean free path means that the lifetime of electrons is the shortest near E_F in the localization regime, violating graphene’s ordinary Fermi liquid behavior [21]. Such an unusual behavior has also been experimentally observed in graphene dosed with a high concentration of H atoms [13].

Near E_F , the mean free path l is much less than the average distance between vacancies (d). This is because the *quasi*-localized states substantially reduce l in the low-energy region. For example, when $x = 0.1\%$, l is found to be 1.6 nm, while d is in the order of 5 nm. In

Fig. 4(b), we plot l as a function of x , which shows that l scales with x in a power law $l = Ax^\delta$ ($\delta = -0.5$) at E_F . Fitting the simulation data, we obtained the parameter $A = 0.508$ nm. This power-law scaling has been derived before from the full self-consistent Born approximation (FSBA) [7], but the FSBA is limited to extremely low concentration and can not describe the localization behavior near E_F and give the quantitative values of l .

Our quantitative results indicate that vacancies are short-range disorders similar to H atoms in graphene as suggested by a recent experiment [13]. The similar results between vacancy defect and H impurity can be understood by the dramatic reconstruction of the energy spectrum near the Dirac point in both cases, while the Fermi energy is preserved. As short-range local scatters, both vacancy and H lead to strong localization by significant scattering. We note that at low defect/impurity concentration, the mean free path l is shorter for vacancy (1.6 nm at $x = 0.1\%$) than for H atom ($\sim 4 - 5$ nm at $x = 0.1\%$). This is because vacancy produces a much stronger local scattering center (creating an infinite barrier) than H (inducing a structural transition from sp^2 to sp^3 hybridization). However, we find that the rate of l decreases faster with x for H ($\delta < -1$) [13] than that for vacancy ($\delta = -0.5$). This is possibly because the scattering center produced by vacancy is more localized limited to single atomic site, while the scattering center produced by H atom is relatively more extended as the sp^3 hybridization induces reconstruction in the neighboring atoms around it. Consequently, at high concentration, multiple scattering by H atoms becomes more and more important, leading to a faster decay of l . A different case was shown in graphene substituted with boron or nitrogen, where the long-range scattering is induced by chemical disorder with $\delta = -1$ [18].

In conclusion, the criticality of vacancy-induced MIT in graphene has been investigated with quantitative simulations. The MIT is shown to occur at the critical vacancy concentration $x_c \approx 0.053\%$, caused by the vacancy-induced *quasi*-localization. Several unconventional critical behaviors have been revealed in the defected graphene with vacancies, including the power-law rather than logarithmic scaling relation between conductivity and diffusion length and the existence of a minimum conductivity at the mobility edge that differs from the universal value of $0.628e^2/h$ expected in conventional 2D localiza-

tion systems. Our results for vacancies are consistent with the most salient features of the H-dosing-induced MIT in graphene as observed in recent experiments [13], suggesting that both vacancy and H belong to the same class of short-range disorders in graphene with H dosing involving stronger multiple scattering. Our studies also shed some new lights to the general understanding of critical behaviors of 2D disordered systems.

* E-mail: fliu@eng.utah.edu

- [1] K. S. Novoselov *et al.*, Science **306**, 666 (2004).
- [2] A. K. Geim and K. S. Novoselov, Nat. Mater. **6**, 183 (2007); B. Oezylmaz *et al.*, Appl. Phys. Lett. **91**, 192107 (2007); B. Oezylmaz *et al.*, Phys. Rev. Lett. **99**, 166804 (2007); Z. Jiang, Y. Zhang, H. L. Stormer, and Ph. Kim, Phys. Rev. Lett. **99**, 106802 (2007); Y. Zhang *et al.*, Phys. Rev. Lett. **96**, 136806 (2006); K. S. Novoselov *et al.*, Nature (London) **438**, 197 (2005); Y. Zhang *et al.*, Nature (London) **438**, 201 (2005).
- [3] K. S. Novoselov *et al.*, Science **315**, 1379 (2007).
- [4] E. McCann *et al.*, Phys. Rev. Lett. **97**, 146805 (2006); H. Suzuura and T. Ando, J. Phys. Soc. Jpn. **75**, 024703 (2006); V. I. Falko *et al.*, Solid State Commun. **143**, 33 (2007); F.W. Tikhonenko *et al.*, Phys. Rev. Lett. **100**, 056802 (2008).
- [5] A. Hashimoto *et al.*, Nature **430**, 870 (2004).
- [6] V. M. Pereira *et al.*, Phys. Rev. Lett. **96**, 036801 (2006).
- [7] N. M. R. Peres *et al.*, Phys. Rev. B **73**, 125411 (2006).
- [8] V. M. Pereira *et al.*, Phys. Rev. B **77**, 115109 (2008).
- [9] B. Huang, *et al.*, Phys. Rev. B **77**, 153411 (2008).
- [10] S. Wu *et al.*, Phys. Rev. B **77**, 195411 (2008).
- [11] J. J. Palacios *et al.*, Phys. Rev. B **77**, 195428 (2008).
- [12] A. L. C. Pereira *et al.*, Phys. Rev. B **78**, 125402 (2008)
- [13] A. Bostwick *et al.*, Phys. Rev. Lett. **103**, 056404 (2009)
- [14] P. A. Lee and T.V. Ramakrishnan, Rev. Mod. Phys. **57**, 287 (1985).
- [15] P. W. Anderson, Phys. Rev. **109**, 1492 (1958).
- [16] S. Roche, Phys. Rev. B **59**, 2284 (1999); F. Triozon *et al.*, Phys. Rev. B **65**, 220202(R) (2002); T. Markussen, "Quantum transport calculations using wave function diffusion and the Kubo formula", Master Thesis in Technical University of Denmark (2006); J.-C. Charlier, X. Blase, and S. Roche, Rev. Mod. Phys. **79**, 287 (2007).
- [17] A. Lherbier *et al.*, Phys. Rev. Lett. **100**, 036803 (2008).
- [18] A. Lherbier *et al.*, Phys. Rev. Lett. **101**, 036808 (2008).
- [19] F. Triozon *et al.*, Phys. Rev. B **69**, 121410(R) (2004).
- [20] S. Roche and D. Mayou, Phys. Rev. Lett. **79**, 2518 (1997).
- [21] A. Bostwick *et al.*, Nature Phys. **3**, 36 (2007).